RSC Advances

ROYAL SOCIETY OF CHEMISTRY

www.rsc.org/advances

Cite this: DOI: 10.1039/c0xx00000x

www.rsc.org/xxxxxx

ARTICLE TYPE

Aminomethylpyrene-based Imino-Phenol as Primary Fluorescence Switch-on Sensors for Al^{3+} in Solution and in Vero Cells and their Complexes as Secondary Recognition Ensemble toward Pyrophosphate

Ajit Kumar Mahapatra*,[a] Syed Samim Ali,[a] Kalipada Maiti,[a] Saikat Kumar Manna,[a] Rajkishor Maji,[a] Sanchita Mondal,[a] Md. Raihan Uddin,[b] Sukhendu Mandal [b], Prithidipa Sahoo[c]

Received (in XXX, XXX) Xth XXXXXXXXX 20XX, Accepted Xth XXXXXXXXX 20XX
DOI: 10.1039/b000000x

Three aminomethylpyrene-based salicyl-imines, viz. **L1**, **L2** and **L3** were synthesized and characterized and their recognition of biologically relevant M^{n+} ions was studied. These three receptors were shown to be selective and sensitive for Al^{3+} among the 13 metal ions studied in HEPES buffer medium by fluorescence, absorption, and visual emission color change with detection limits of 3.60, 2.13 and 2.16 μM, respectively, by **L1**, **L2** and **L3**. The interaction of Al^{3+} with three receptors (**L1**, **L2** and **L3**) have been further supported by absorption studies, and the stoichiometry of the complex formed (1:1) has been established on the basis of emission and ESI-MS. Competitive ion titrations carried out reveal that the Al^{3+} can be detected even in the presence of other metal ions of bio importance. The structure of the aluminium complexes and their mode of interactions were established by DFT calculations. TDDFT calculations were performed in order to demonstrate the electronic properties of receptors. Microstructural features of **L2** and its Al^{3+} complex have been measured by AFM. Moreover, the utility of the receptors **L1**, **L2** and **L3** in showing the aluminium recognition in live cells has also been demonstrated using Vero cells as monitored by fluorescence imaging. In situ prepared **[AlL1]** and **[AlL3]** complexes were found to be sensitive and selective toward phosphate-bearing ions and molecules and in particular to pyrophosphate (PPi) among the other 15 anions studied; however, [**AlL2**] was not sensitive toward any of the anions studied.

Introduction

The development of fluorescent sensors for ubiquitous cations and anions in nature has been a recent area of focus due to their potential applications in environmental detection, molecular catalysis, medicine and the monitoring of biological processes.[1-3] In particular, the development of a fluorescent probe for aluminum ion in the presence of a variety of other metal ions has received great attention due to widespread application of aluminum in modern life.[4] However, excess aluminum can cause damage to certain human tissues and cells, resulting in diseases such as Dementia and Encephalopathy, Alzheimer's[5] and Parkinson's diseases[6] and are believed to be attributed to the toxicity of Al^{3+}. Also, Al^{3+} causes neurofibrillary, enzymatic, and neurotransmitter changes in the central nervous system. Aluminum accumulation has been shown to cause cancer of the lung, breast, and bladder.[7] Aluminum may also directly affect iron metabolism by influencing the absorption of iron via the intestine, hindering iron transport in the serum, and displacing iron by binding to transferring.[8] The increase of Al^{3+} concentration in the environment due to acidic rain and human activities is deadly for growing plants.[9] High concentration of Al^{3+} hampers plant performance,[10] killing fish, algae, bacteria, and other species in aquatic ecosystems.[11] The WHO recommended the average daily human intake of Al^{3+} of around 3–10 mg and weekly tolerable dietary intake as 7 mg kg^{-1} body weight.[12] Therefore, the facile detection of Al^{3+} is crucial in environmental monitoring and biological assays, and remains a major requirement. However, compared to other transition metal ions, limited examples of fluorescence sensors based on small molecules for Al^{3+} have been reported.[13]

Al^{3+} is also associated with various anions, especially with phosphates, owing to its strong chelation as well as bridging capability. Phosphate-based inorganic as well as organic molecules play fundamental roles in a wide range of chemical and biological processes of human life. Among the phosphates (Pi), inorganic pyrophosphate (PPi) is a particular interest due to an essential anion for normal cellular functioning and has numerous other applications in biology as well as in the environment.[14] In addition, PPi has also been used as an additive in foods.[15] The accumulation of the PPi complex of Ca^{2+} in the fluid of joints is indicative of the disease that is popularly known as calcium pyrophosphate deposition disease (CPDD).[16] Therefore, the selective detection of PPi has been a major

research focus. Although traditional methods of anion sensing such as the use of ion-selective electrodes have already been discovered, there is an increasing need to find alternative means of analysis, including the use of selective fluorescent chemosensors.[17] In general, sensing of anions in aqueous system is much more challenging task than cation due to the strong hydration effects of anions. Recently, metal ion complexes have been used as receptors for phosphates, and this emerged as one of the most successful strategies, since it provides specific metal ion-anion interactions.[18] In this regard, metal ion complexes are ideal binding sites for PPi recognition rather than hydrogen bonding interaction in aqueous or organo-aqueous solutions. So, the utilization of a metal ion complex as a binding site for PPi has been found to be the most successful strategy because the strong binding affinity between metal ions and PPi allows the detection of PPi in 100% aqueous solutions. To date, these studies frequently have adopted the fluorescent complexes containing a metal cation (such as Al^{3+}) chelator coupled with a variety of chromophores.[19]

In our recent publication, we have demonstrated the selective detection of anions using C_3-symmetry tri-arm 8-hydroxyquinoline based conjugates bearing metal ion ensemble.[20] Therefore, it is of prime interest to develop chelating ligand-based molecular systems to provide better sensitivity and selectivity toward ions and molecules. Thus, in present paper, the synthesis and characterization of imino-phenolic-pyrene conjugates **L1**, **L2** and **L3**, and their chemoensembles that formed upon binding of Al^{3+} to **L1**, **L2** and **L3**, viz., **[AlL1]**, **[AlL2]** and **[AlL3]**, have been explored extensively to sense PPi selectively among common biological phosphates. The selection of salicyl-OH and imine moieties in the designed chemosensor are based on the considerations that it can function both as a fluorescent quencher and as the potential binding unit for metal ions.[21] For a sensor based on the phenolic Schiff base molecular systems, fluorescence is quenched via owing to the isomerization of the imine (C=N bond) as well as to the excited-state proton transfer (ESPT) from salicyl (−OH) to the imine nitrogen in the excited state. Upon complexation with a suitable metal ion, a large chelation-enhanced-fluorescence (CHEF) effect is observed. In the mean time, when a fluorophore contains an electron-donating group (often an amino group) e.g. **L2** conjugating to a fluorophore, it undergoes ICT from the donor to the fluorophore upon light excitation. If a cation promotes the electron-donating character of the electron donor group, the absorption and fluorescence spectra should be red-shifted. The extended−conjugation enhanced the intramolecular charge transfer (ICT), which is expected to be highly sensitive towards external perturbations such as metal ion proximity resulting into optical and spectral changes. So, we expected that the combination of these two parts donor and binding moieties in common platform would generate a novel sensor with high selectivity and sensitivity for aluminium and PPi ions.

Experimental Section

General Information and Materials. The ^1H and ^{13}C NMR spectra were recorded on a Bruker AM-400 spectrometer using Me_4Si as the internal standard. The ^1H NMR chemical shift values are expressed in ppm (δ) relative to $CHCl_3$ (δ = 7.26 ppm). Mass spectra were carried out using Water's QTOF Micro YA 263 mass spectrometer. UV–visible and fluorescence spectra measurements were performed on a SHIMADZU UV-1800 and a PerkinElmer LS-55 spectrofluorimeter respectively. DMSO of analytical grade was purchased from Spectrochem. All other materials for synthesis were purchased from Aldrich Chemical Co. and used without further purification. The solutions of anions were prepared from their tetrabutylammonium salts of analytical grade, and then subsequently diluted to prepare working solutions.

Vero cells (very thin endothelial cell) (Vero 76, ATCC No CRL-1587) were used as models. Vero cells were incubated in PBS buffer (pH 7.4) containing 10 μM of the probe (**L2**) for 20 min at 37 °C, followed by washing the cells with the same buffer to remove the excess of the probes. At this stage, the fluorescence microscopy image of Vero cells displayed weak intracellular fluorescence. However, upon the addition of exogenous Al^{3+} into the cells for 20 min at 37 °C.

The AFM samples of **L2**, **[L2+Al^{3+}]** were prepared at $5x10^{-5}$M concentration in ethanol. The receptor **L2** was initially dissolved in 100 µL of $CHCl_3$ and then made up with ethanol to the desired concentration. The stock solutions of these were sonicated for 20 mins. Then 50-100 µL of aliquot was taken from this stock solution to spread over mica sheet using the drop cast method. The samples were then dried and analyzed by AFM technique.

Preparation of Test solution for UV-vis and fluorescence study. A stock solution of the probe **L1, L2 and L3** (2.0×10^{-5} M) were prepared in DMSO:H_2O (2:1). In titration experiments, each time a 2×10^{-5} M solution of **L1, L2 and L3** were filled in a quartz optical cell of 1 cm optical path length, and the ion stock solutions were added into the quartz optical cell gradually by using a micropipette. Spectral data were recorded at 1 min after the addition of the ions. In selectivity experiments, the test samples were prepared by placing appropriate amounts of the ions (4×10^{-4} M) stock into 2 mL of solution of **L** (2×10^{-5} M).

Computational Studies. All geometries for **L1, L2, L3** and **[AlL1], [AlL2], [AlL3]** were optimized by density functional theory (DFT) calculations using Gaussian 09 [B3LYP/6-31G(*d*)] software package.

Synthesis and characterization of L1:

The synthetic route of **L1**, **L2** and **L3** is shown in (scheme1). An ethanolic solution (3 mL) of pyrenemethylamine (250 mg,1.0 mmol) was added to another ethanolic solution (3 mL) of salicylaldehyde (122.0 mg, 1.0 mmol). The mixed solution was refluxed for 4 hrs and then cooled to room temperature. A yellow

precipitate was appeared, filtered, washed with EtOH for several times and then dried under vacuum. Then we got target product salicylaldehyde pyrenemethylamine schiff-base (**L1**) which was dried under vacuum. The conjugate **L2** and **L3** were synthesized by adopting the similar procedure.

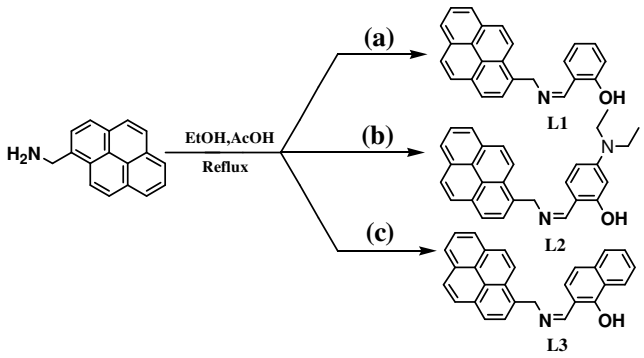

Scheme 1. Synthesis of the probe **L1**, **L2** and **L3**.

Reagents*:* (a) Salicylaldehyde; (b) 4-N,N-diethyl amino salicylaldehyde; (c) 1-hydroxy-2-naphthaldehyde.

Results and discussion

The chemosensing ensembles were prepared by mixing a 1:2 mol ratio of chemosensors **L1/L2/L3** and Al^{3+} in the 1 : 2 v/v HEPES buffer/ethanol mixture at pH = 7.4 (referred to hereafter as "aqueous buffer solution), and these are used for all the studies with anions reported in this paper.

Prior to being applied in the fluorescence sensing of anions, the binding interaction of chemosensors **L1**, **L2** and **L3** with metal ions were first studied by UV-vis absorption and fluorescence spectroscopy. The sensitivity of **L1**, **L2** and **L3** toward different metal ions and their preferential selectivity toward Al^{3+} over the other ions has been studied by fluorescence titrations.

The absorption spectra of free **L1**, **L2** and **L3** in aqueous DMSO (1:2; v/v) HEPES buffer (pH 7.4) exhibited different bands from 200 to 400 nm and these spectra are typical of a poly aromatic compound, the absorption arises mainly due to π–π^* transitions of the signaling subunit.

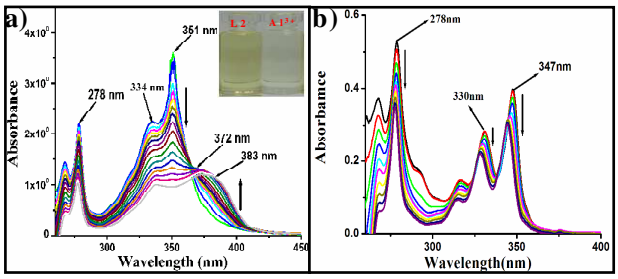

Figure 1. (a) UV-vis spectral changes of L2 (2.0 x10^{-5} M) in DMSO-H_2O (2:1, v/v; pH 7.4) upon addition of Al^{3+} (4.0 x10^{-4} M).The inset shows naked eye color change of L2 and addition of Al^{3+} in DMSO-H_2O (2:1; V/V; pH 7.4). (b) UV-vis spectral changes of L1 (2.0 x10^{-5} M) in DMSO-H_2O (2:1, v/v; pH 7.4) upon addition of Al^{3+} (4.0 x10^{-4}M).

Upon the addition of Al^{3+} to a solution of **L1**, **L2** and **L3** separately in DMSO-water brought changes absorption spectra with common three absorption bands observed at ~278, ~330 and ~350 nm. When **L1** (Figure.1b) and **L2** (Figure.1a) were titrated against Al^{3+}(0-10 equiv), a significant decrease in the bands at 278, 330 and 350 nm and a new band was observed at ~383 nm in case of **L2**, and its absorbance increases with observation of an isosbestic point at 372 nm. The band at ~383 nm could be attributed to the intramolecular charge transfer transition from the donating diethylamino group to the imino-phenolic binding zone which acts as an acceptor during complexation, indicating the formation of the **[AlL2]** ensemble. The low energy (LE) band for **L2** at 350 nm was gradually decreases, upon addition of Al^{3+} ions, which is responsible for the change of colour from yellow to colourless. This fact can be used for a 'naked-eye' detection of Al^{3+} ions.

The chemosensors **L1**, **L2** and **L3** exhibit very weak emission in the range 350-500 nm when excited at 330, 351 and 330 nm respectively. All of the studies were carried out in DMSO-H_2O (2:1) mixture at pH 7.4 to have an effective HEPES buffer concentration of 0.4 mM by maintaining the ligand concentration of 20 μM throughout the experiment and varying the mole ratio of the added metal ion. Titration of **L1** (Figure.2a), **L2** (Figure.2b) and L3 (Figure.S19, †) with Al^{3+} results in the enhancement of fluorescence intensity as a function of the added Al^{3+} concentration.

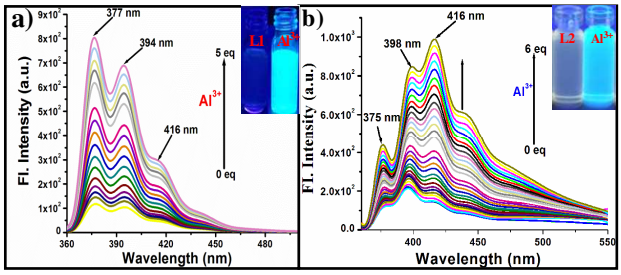

Figure 2. (a) Fluorescence changes of **L1** (2.0 x10^{-5} M) in DMSO-H_2O (2:1; v/v; pH 7.4) upon addition of Al^{3+} (4.0 x10^{-4} M).The inset shows naked eye color change of **L1** and addition of Al^{3+} in DMSO-H_2O (2:1, v/v ; pH 7.4). (b) Fluorescence changes of **L2** (2.0 x10^{-5} M) in DMSO-H_2O (2:1, v/v ; pH 7.4) upon addition of Al^{3+} (4.0 x10^{-4} M). The inset shows naked eye color change of **L2** and addition of Al^{3+} in DMSO-H_2O (2:1, v/v ; pH 7.4).

However, upon the progressive additions of Al^{3+} (0–5 equiv.) to the solution of **L1** distinct fluorescent enhancement with dual emission bands centred at 377 and 394 nm were observed and a third weak band was observed at ~416 nm (Figure. 2a). On the other hand **L2** also showed dual emission bands at 375 and 398 nm upon similar additions of Al^{3+} along with a strong third emission band at 416 nm was observed (Figure. 2b). As for **L3**, it exhibits similar fluorescence responses as good as for **L1** during the interaction with Al^{3+} (Figure.S19, †).

This fluorescence enhancement could be explained by an excited state intramolecular proton transfer (ESIPT) mechanism, C=N

isomerization, and chelation enhanced fluorescence (CHEF) (Scheme 2).

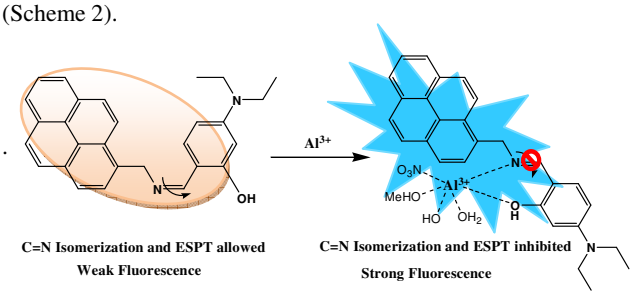

Scheme 2. Schematic presentation of Al^{3+}binding mode with **L2**.

When chemosensors **L1**, **L2** and **L3** exists as an unbound form, they exhibit weak fluorescence owing to the isomerization of the imine (C=N bond) as well as to the excited-state intramolecular proton transfer (ESIPT) from salicyl –OH to the imine nitrogen.[22] In the excited state, which has been well documented in the literature in the case of Schiff base molecular systems.[23] By contrast, upon addition of Al^{3+} to chemosensors, a stable chelation by Al^{3+} to the imine nitrogen and phenolic oxygen brings rigidity to the conjugates and generating efficient chelation enhanced fluorescence (CHEF).[24] Plot of relative fluorescence intensity (I/I_0) versus **[Al^{3+}]/[L]** mole ratio suggests the formation of a 1:1 complex in each case and hence is stoichiometric.

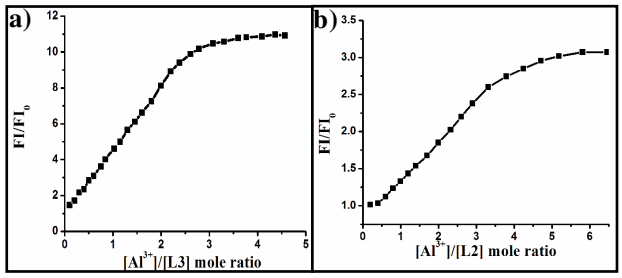

Figure 3. (a) Change in fluorescence intensity (λ_{ex}= 331 nm) ratio (FI/FI_0) (at 377 nm) vs **[Al^{3+}]/[L3]** mole ratio. (b) Change in fluorescence intensity (λ_{ex}= 351 nm) ratio (FI/FI_0) (at 416 nm) vs **[Al^{3+}]/[L2]** mole ratio.

The binding affinities of Al^{3+} toward **L1**, **L2** and **L3** have been calculated from the Benesi–Hildebrand equation and found to have binding constants 2.0×10^4 M, 4.1×10^4 M and 1.9×10^4 M (Figure. S15, S16, S17 respectively and Table S1, †) respectively. Higher binding constant observed in the case of **L2** as compared to **L1** and **L3** speaks for the stronger binding of Al^{3+} with **L2**, as explained on the basis of the tight coordination due to enhanced intramolecular charge transfer (ICT) from electron donor diethylamino group to binding zone.

In order to check whether **L1**, **L2** and **L3** are sensitive to only Al^{3+} or even to the other ions, competitive titrations were carried out in the presence of other biologically and ecologically relevant metal ions. In the fluorescence titration, the result found, none of these metal ions significantly affect the emission intensities of **L1** (Figure. S21, †), **L2** (Figure.3a) and **L3** (Figure.4b) upon the addition of Al^{3+}, to have only marginal changes in the emission intensity, suggesting that none of these ions interfere in the fluorescence emission of the Al^{3+} complex. Therefore, it can be concluded that **L1**, **L2** and **L3** recognizes Al^{3+} even in the presence of other metal ions. Fluorescence titrations were carried out in the same medium for **L2** with 12 different metal ions, viz. Mg^{2+}, Cu^{2+}, Zn^{2+}, Ni^{2+}, Co^{2+}, Fe^{3+}, Ca^{2+}, Hg^{2+}, Cd^{2+}, Au^{3+}, Mn^{2+}, Cr^{3+}, found no significant fluorescence enhancement except Au^{3+}, Cr^{3+} and Fe^{3+} revealed relatively insignificant fluorescence ON responses in this region (Figure.4). This might be due to their paramagnetic properties which promote dissipation of the excited state energy in a non-radiative process as a result of spin–orbital coupling.[25]

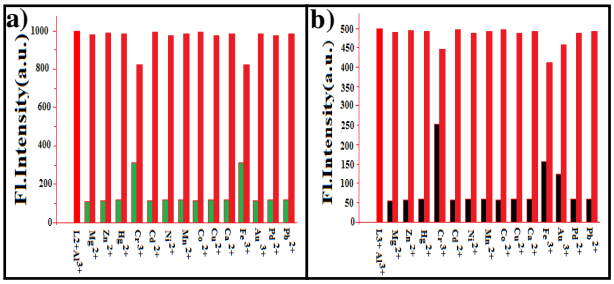

Figure 4. (a) Competitive graph; green bar: **L2** + cations (5 equiv.), red bar: **L2** + cations (5 equiv.) + Al^{3+}(3 equiv.). (b)Competitive graph; black bar: **L3** + cations(5 equiv.), red bar: **L3** + cations(5 equiv.) + Al^{3+}(3 equiv.).

Therefore, **L1**, **L2** and **L3** can be used for the selective recognition of Al^{3+} among the 12 different metal ions studied. Minimum detectable concentrations of **L1**, **L2** and **L3** are 3.6 μM, 2.01 μM and 2.16 μM (Figure. S11, S12, S13 respectively and Table S1, †) respectively, has been detected by the fluorescence titrations carried out by keeping the receptor to Al^{3+} mole ratio as 1:1.

To be useful in biological applications, it is necessary for a fluorescent probe to operate over a suitable range of pH, especially at physiological pH. A series of buffers with pH values ranging from 1 to 13 was prepared by mixing sodium hydroxide solution and hydrochloric acid in HEPES buffer.

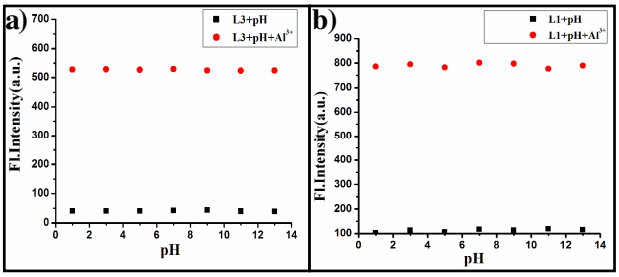

Figure 5. (a)Change in fluorescence intensity (λ_{ex}= 331 nm) of **L3** (at 377 nm) with different pH (black dots) and with the addition of Al^{3+} in to it(red dots). (b) Change in fluorescence intensity (λ_{ex}= 331 nm) of **L1** (at 377 nm) with different pH (black dots) and with the addition of Al^{3+} in to it(red dots).

Thus, we proceeded to investigate the effect of pH on the fluorescence intensity of the probe **L1** (Figure. 5b) in absence or presence of Al^{3+}. The results showed that fluorescence intensity (I_{377} nm) of **L1** showed no apparent changes in the pH range from 1.0 to 13.0 no matter with or without Al^{3+}, indicating that **L1** is stable and its response towards Al^{3+} was also almost invariable in this pH range .Similar effect of pH was observed in case of **L2** (Figure. S18, †) and L3 (Figure. 5a).

ESI mass spectra obtained for in situ complexes of **L1**, **L2** and **L3** with Al^{3+} resulted in molecular ion peaks at (m/z) 536.1729 (calc. 536.1713), 563.0363 (calc. 564.2639) and 541.1962 (Calc.541.1964) respectively (Fig. S3, S7, and S10 respectively, †). The mass spectra are assignable to the mass of [**L1**+Al+$(NO_3)_2$+MeOH+H_2O]$^+$, [**L2**+Al+(NO_3)+MeOH+H_2O +OH]$^+$ and [**L3**+Al+NO_3+MeOH+H_2O+OH]$^+$ supports the presence of aluminium. Therefore, we suggest that probes **L1, L2** and **L3** coordinates with Al^{3+} with 1:1 stoichiometry.

In addition, we investigated the ^{1}H NMR spectra of **L2** in the presence of Al^{3+}. The addition reaction of Al^{3+} to **L2** was confirmed by the comparison of ^{1}H NMR spectra of **L2** with and without the addition of Al^{3+} in DMSO-d6 (Figure. 6).

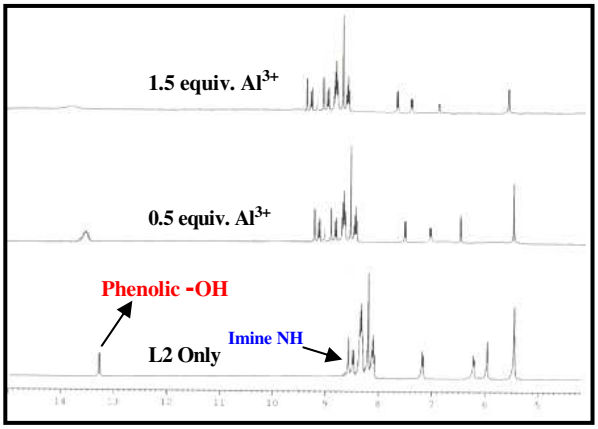

Figure 6. ^{1}H NMR chart (400 MHz, DMSO-d_6 , 0.5 ml) of **L2** (10 mg) measured with different equivalent of Al^{3+}.

From NMR titration it is found that the peak corresponding to phenolic-OH proton gets broadened and both the phenolic-OH and imine-CH at 13.76 ppm and 8.56 ppm respectively get shifted downfield with the gradual addition of Al^{3+} ion. This clearly indicates that Al^{3+} is being coordinately bound with both phenolic oxygen and imine nitrogen atom.

To verify the structural features of the probes **L1**, **L2** and **L3**, their aluminium complexes **[AlL1], [AlL2], [AlL3]** were addressed by computational studies.[28-29] The geometry optimizations for probes (**L1**, **L2** and **L3**) (Figure.S28a, S26a, and S30a, †) and their complexes (Figure.7) were done in a cascade fashion starting from semiempirical PM2 followed by *ab initio* HF to DFT B3LYP by using various basis sets, *viz.*, PM2 → HF/STO-3G → HF/3-21G → HF/ 6-31G → B3LYP/ 6-31G(d). For optimization of the complexes, a starting model was generated by taking the DFT optimized probes (**L1**, **L2** and **L3**) and placing the Al^{3+} ion well in the core of the pyrene enamine nitrogen and phenolic (–OH) as donors moieties at a non-interacting distance. The optimized complexes were mainly formed through the interaction of imine nitrogen and phenolic oxygen atom of probes (**L1**, **L2** or **L3**) leads to distorted geometries by exhibiting coordination bond length in the range with N_1–Al = 1.90 Å and O_1–Al = 2.10 Å (for **L1**), N_2–Al = 1.92 Å and O_2–Al = 2.14 Å (for **L2**), N_3–Al = 1.91Å and O_3–Al = 2.09 Å (for **L3**), (Figure.S28b, S26b, and S30b, †)

The spatial distributions and orbital energies of HOMO and LUMO of probes (**L1**, **L2** and **L3**) and their corresponding aluminium complexes **[AlL1], [AlL2]** and **[AlL3]** were also determined to explain the change of electronic properties of these complexes in their ground and excited states. The vertical transitions calculated by TDDFT (Table S5, S3, S7, †) were compared with the UV–vis spectra of **[AlL1]**, **[AlL2]** and **[AlL3]** were found to have good agreement with the experimental data.

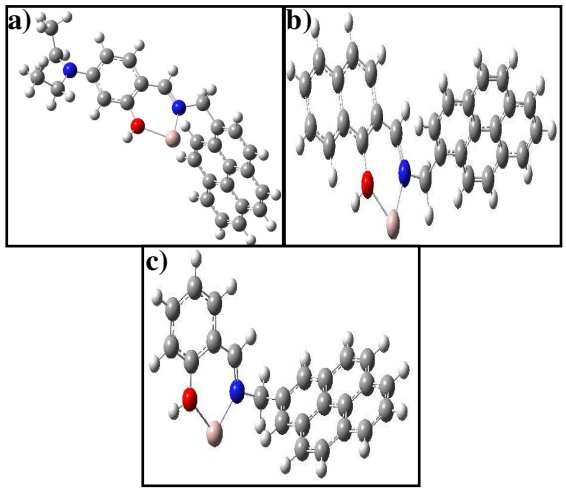

Figure 7. Energy minimization structure of (a) **[AlL2],** (b)**[AlL3]** and (c) **[AlL1].**

The TDDFT calculations performed at the B3LYP/6-31G (d) level of theory revealed the absorption bands in the region of λ_{max} 250–400 nm. These study suggest that the vertical transitions observed at ~344 and ~331 nm, ~372 and ~350 nm, ~330 nm and ~345 are comparable with those from experimental data for **[AlL1], [AlL2]** and **[AlL3]** respectively. In all cases, the highest observed oscillator strengths (F) correspond to the experimental λ_{max} (at ~351, ~347 and ~331 nm), that results from π→π* of the salicylimine and pyrene fragments of the probes . The π electrons on the relevant HOMOs and LUMOs of **[AlL1], [AlL2]** and **[AlL3]** complex are essentially distributed in the entire salicylimine and pyrene backbone respectively. By contrast, in the case of **L1**, the π electrons on HOMO and HOMO–1 are primarily resided on the π-conjugated pyrene moiety. Corresponding molecular orbitals (MOs) of the three complexes for one electron excitations are shown in (Figure. S29, S27, S31,†) . Moreover, the HOMO–LUMO energy gaps of complexes **[AlL1], [AlL2]** and **[AlL3]** becomes much smaller

relative to their probes **L1**, **L2** and **L3**. The energy gaps between HOMO and LUMO in the probes and their complexes were shown in the supplementary information portion (Table S4, S2 and S6, †).

In order to understand how the microscopic structural features of the probe **L2** changes from its in situ complexes **[AlL2],** the atomic force microscopy (AFM) technique was used. **L1**, **L2,** and **L3** exhibit very similar recognition properties towards Al^{3+}. Hence it was postulated that the microstructure of a representative sample **[AlL2]** would provide a reliable indication of the change in physical properties experienced by **L1** and **L3** due to interaction with Al^{3+}.

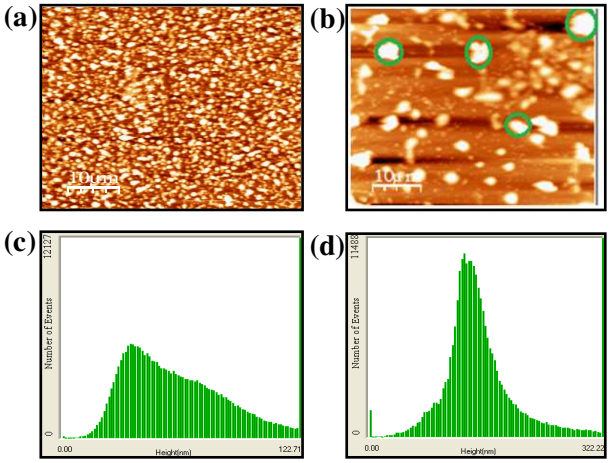

Figure 8. AFM micrographs of (a) **L2** and (b) **[Al^{3+}–L2].** Few representative lumps are encircled on (b). RMS roughness observed in AFM for **L2** in the absence (c) and in the presence (d) of Al^{3+} ion.

The AFM images of the probes **L2** and its complexes show that the particles were well spread over the mica sheet. The morphological feature of L2 is quite different from their respective complexes. While complexes forms large lumps, like aggregates of size 150 to 240 nm, such aggregation is not present in the probes **L2** only. However, the probes **L2** is uniformly distributed over the mica sheet with an average size of 90 to 140 nm. The formation of larger particles in **[AlL2]** is attributable to the Al^{3+} induced agglomerations of the probes (Figure. 8).

Owing to the strong affinity of Al^{3+} toward the phosphate, the highly switch on fluorescence with large fold enhancement of Al^{3+} complexes **[AlL1]** and **[AlL3]** have been studied for their secondary sensing property toward phosphate-based anions. Therefore, the in-situ prepared aluminium complexes in aqueous buffer solution have been used as chemo-sensing ensembles for anions.

The recognition behavior of the *in situ* prepared ensemble Al^{3+} complexes **[AlL1]** and **[AlL3]** have been evaluated by carrying out the fluorescence titrations of **[AlL1]** and **[AlL3]** in aqueous buffer solution at pH 7.4 with different anions, viz., F^-, Cl^-, Br^-, I^-, NO_3^-, SO_4^{2-}, AcO^-, HSO_4^-, $H_2PO_4^-$, (Pi), $P_2O_7^{4-}$, (PPi) as well as nucleotides. Fluorescence of **[AlL3]** has been quenched gradually in the case of inorganic pyrophosphate (PPi), and the complete quenching was observed at ~10 equivalent owing to its strong binding nature toward Al^{3+}. The fluorescence intensity of **[AlL3]** complex was decreases regularly with increasing concentration of PPi as shown in the inset of (Figure.9a). Unlike the strong fluorescence decrease observed upon the addition of PPi, the other phosphate based anions such as Pi showed moderate fluorescence changes that too at higher mole ratios. This clearly suggests that the **[AlL1]** (Figure.S33, †) and **[AlL3]** (Figure. 9b) are sensitive chemo-sensing ensemble for phosphate based anions, particularly, to the PPi, among the different anions studied in aqueous buffer solution (Figure. 9b). The selectivity for PPi over other anions can be attributed to a strong coordination of Al^{3+} to the phosphate unit, which was also explained by Yoon and Hong.[26]

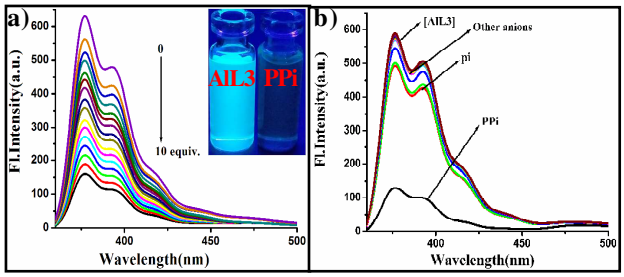

Figure 9. (a) Fluorescence spectral change of **[AlL3]** in DMSO-H_2O (2:1,v/v) in HEPES buffer (20 mM, pH 7.4) with the gradual addition of PPi. Inset shows the fluorescence color change of **[AlL3]** with the addition of PPi. (b) Competitive fluorescence spectra of **[AlL3]** with different anions in DMSO-H_2O (2:1, v/v) in HEPES buffer (20 mM, pH 7.4)

The visual color changes from blue fluorescent to nonfluorescent in the presence of PPi that is similar to that of the **L3**, while all the other anions show no change in the color (Figure. 9a inset). The sensitivity of **[AlL3]** for PPi has been evaluated by measuring the detectable lowest concentration. The fluorescence titration carried out between **[AlL3]** and [PPi] by maintaining a 1:1 ratio resulted in 6.4 μM of PPi as the lowest detectable concentration in aqueous buffer medium (Figure.S15, †). The **[AlL2],** which is contained of one electron donating NEt_2 moiety in the phenyl ring as compared to **[AlL3],** does not show any significant fluorescence change toward any of these anion; however, **[AlL2]** shows small quenching of fluorescence intensity in the case of almost all the phosphate ions due to electron donating character of -NEt_2 group increases electron density in the binding core. This is attributable to the binding of phosphate due to interaction between PPi and **[AlL3]** followed by the removal of Al^{3+} in the form of **[Al•PPi]**, thus releasing the free **L3**. Thus the [**AlL3**] complex acts as a secondary recognition ensemble toward PPi. Removal of Al^{3+} bound to the Schiff's base core by the phosphate has been reported in the literature.[27]

In general, molecules can undergo changes in the ground or excited states, in response to modulators which can be guest molecules, ions, or light of a certain wavelength. In most cases, these changes could then be signaled by changes in the emission

intensity, or wavelength shift. Due to similar sensing behaviours of **L1** and **L3**, it is safe to assert that the logic functions characteristic of one of the chemosensors will be faithfully reproduced by the other. So, the fluorescence result describe above for **L1** by monitoring one output at 377 or 394 nm, we used our system for the construction of logic gate INHIBIT (INH) logic functions by using two sets of input signals, while one is Al^{3+} and the other is PPi. Without any chemical input, free compound **L1** did not show any strong emissions at 377 nm. With respect to inputs, the presence and absence of $Al^{3+}$and PPi are defined as ''1'' and ''0'', respectively. Additionally, we define the fluorescence high and low signal as outputs ''1'' and ''0'', respectively. From the logic gate functions, the emission of **L1** is observed only in the presence of single input, *viz*., Al^{3+} and not with PPi and Pi as these phosphates are insensitive to **L1**. This indicates that **L1** is switched on only in the presence of Al^{3+} at 377 nm.

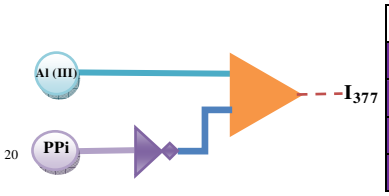

Al(III)	PPi	I_{377}
0	0	0
1	0	1
0	1	0
1	1	0

Figure 10. Truth table and symbolisation of a complementary output INH circuit.

Similarly, in the presence of PPi fluorescence emission of [**AlL1**] was quenched and no significant output signal was observed. From these studies, it has been found that **L1** can be used as INH logic gate toward Al^{3+} in the absence of PPi by observing emission at 377 nm. The two-input Al^{3+} and PPi mimics the performance of INH logic gate by observing emission at 377 nm. The truth table and the pictorial representation for the corresponding INH logic gate are given in Figure 10.

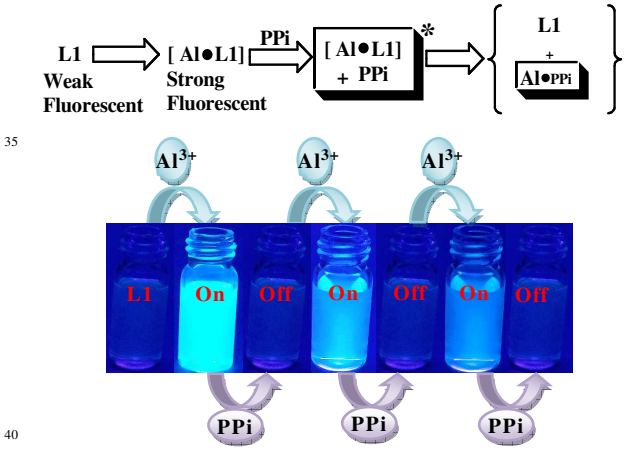

Figure 11. Fluorescence experiment showing on–off reversible visual fluorescence color changes of **L1** after each addition of Al^{3+} and PPi sequentially.

The reversibility is an important aspect of any receptor to be employed as a chemical sensor for detection of specific metal ions. Both **L1** and **L3** showed similar behavior towards PPi, it is safe to assert that the reusability and reversibility of one of the chemosensors will be faithfully reproduced by the other.

So, the reusability of the probe **L1** for sensing Al^{3+} has been demonstrated by carrying out four alternative cycles of the titration of **L1** with Al^{3+} followed by PPi. Al^{3+} shows remarkable switch-on fluorescence changes through formation of **[AlL1]**, and further the titration of this fluorescent complex with PPi quenches the same by removing the Al^{3+} from **[AlL1]** in DMSO-H_2O (2:1, v/v) in HEPES buffer (20 mM, pH 7.4) (Figure.11). The bright bluish fluorescence is immediately turned off. Titration of **[AlL1]** with PPi shows significant switch off fluorescence, and the fluorescence is regained when Al^{3+} is added to result in the switch on mode. Hence, **L1** is a reversible and reusable sensor for Al^{3+} and its complex **[AlL1]** as a secondary sensor for PPi.

To further demonstrate the practical application of the probes, we carried out experiments in living cells. In *vitro* studies established the ability of **L2** to detect Al^{3+} in biological system with excellent selectivity. **L2** is an obvious choice for cellular imaging study due to the presence of the electron donating NEt_2 moiety which helps achieve the strongest analyte binding in case of **L2** among the three sensors studied. This is evident from the binding constants [$2x10^4$ (M), $4.1x10^4$ (M), $1.9x10^4$ (M) for **L1**, **L2**, **L3** respectively].Vero cells (very thin endothelial cell) (Vero 76, ATCC No CRL-1587) were used as models (Experimental Section). However, to materialize this objective it is a prerequisite to assess the cytotoxic effect of probe **L2**, Al^{3+} and the complex on live cells.

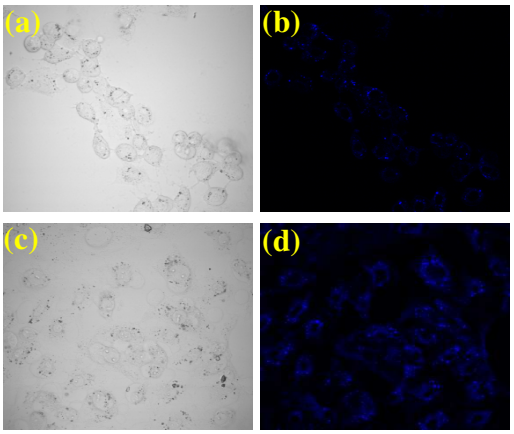

Figure 12. Confocal microscopic images of probe **(L2)** in Vero 76 cells pretreated with Al^{3+} : (a) bright field image of the cells of controlled set. (b) Only Al^{3+} at 1.0×10^{-4} M concentration, nuclei counterstained with DAPI (1 μg mL^{-1}). (c) bright field image of the cells treated with probe **L2** (1.0×10^{-6} M) and Al^{3+} (d) Image scan of probe **L2**(1.0×10^{-6} M) and Al^{3+}. All images were acquired with a 60× objective lens. Scale bar represents 20 μm.

The well-established MTT assay (Figure. S32, †), which is based on mitochondrial dehydrogenase activity of viable cells were

adopted to study cytotoxicity of above mentioned compounds at varying concentrations mentioned in method section. Cytotoxicity measurements for each experiment shows that probes **L2** does not exert any adverse effect on cell viability, same are the cases when cells were treated with varying concentrations of Al^{3+}. Now, Vero cells were incubated in PBS buffer (pH 7.4) containing 10 μM of the probe **L2** for 20 min at 37 °C, followed by washing the cells with the same buffer to remove the excess of the probes. At this stage, the fluorescence microscopy image of Vero cells displayed weak intracellular fluorescence. However, upon the addition of exogenous Al^{3+} into the cells for 20 min at 37 °C, the cells exhibited highly intense blue fluorescence (Figure 12d). The control experiments carried out with Al^{3+} solution alone do not show any fluorescence (Figure 12b). Thus, Vero cells incubated with **L2** in the presence of Al^{3+} showed much greater fluorescence emission as compared to the cells which were not incubated. With this, suggesting that Al^{3+} is responsible for enhancing the fluorescence of **L2** in the cells, as it has also been shown to exhibit fluorescence enhancement in the solution medium. These results clearly indicate that the imino–phenolic–pyrene probe **L2** is effective intracellular Al^{3+} imaging agents with cell permeability.

Conclusion

The imino-phenolic-pyrene probes of **L1**, **L2** and **L3** have been synthesized and characterized. These were found to be sensitive and selective receptors for Al^{3+} in HEPES buffer medium. Their selectivity and sensitivity were demonstrated on the basis of fluorescence, absorption, ^{1}H NMR spectroscopy, ESI mass spectrometry, and visual fluorescent color changes. **L1**, **L2** and **L3** can detect Al^{3+} up to 3.6 µM, 2.13µM, 2.16 µM respectively by switch-on fluorescence, suggesting its applicability to detect Al^{3+} ions in aqueous HEPES buffer medium. TDDFT calculations were performed to demonstrate the electronic properties of **L1**, **L2**, **L3** and their corresponding aluminium complexes. We have found significant similarities with the experimental results. In solution, **[AlL2]** shows strong fluorescence emission at 416 nm when excited at 351 nm through exhibition of an intense blue color fluorescence under UV light. To know the supramolecular microstructural features of **L2** and **[AlL2]** complex, AFM studies were carried out in which the discrete shaped particles of **L2** was found aggregated form in the complex. **L2** was demonstrated as potential live-cell fluorescence imaging agents under microscopy using Vero cells. Weak fluorescent images were observed when Vero cells were incubated with these probes alone. However, strong fluorescence was observed in Vero cells in the presence of Al^{3+}. Hence, these result clearly indicate that the imino-phenolic-pyrene probe, viz., **L2**, is effective intracellular Al^{3+} imaging agents with cell permeability. The in situ prepared fluorescent chemo-ensembles aluminium complexes, viz., **[AlL1]** and **[AlL3],** have been subjected to studies of their secondary sensing properties toward various anions. Owing to this unique features of these complexes have been used as a chemo-ensemble sensor for phosphate based anions in general and PPi in particular among the twelve different anions. These observed fluorescence responses at appropriate monitoring wavelengths could be used as a output signals to demonstrate in principle a basic INH logic gate properties using two inputs. These results will be useful for further molecular design to mimic the function of complex logic gates.

Acknowledgement

We thank the DST-New Delhi [Project file no. SR/S1/OC-44/2012] for financial support. SM thanks to the UGC, New Delhi for a fellowship.

Notes and references

[a]Department of Chemistry, Indian Institute of Engineering Science and Technology, Shibpur, Howrah-711103, West Bengal, India, Email: akmahapatra@rediffmail.com, Fax: +913326684564

[b]Department of Microbiology, University of Calcutta, Kolkata- 700019. \

[c]Department of Chemistry, Visva-Bharati (A Central University), Santiniketan 731235, India.

† Electronic Supplementary Information (ESI) available: [details of any supplementary information available should be included here]. See DOI: 10.1039/b000000x/

1 X. Chen, Y. Zhou, X. Peng and J. Yoon, *Chem. Soc. Rev*., 2010, **39,** 2120.

2 Z. Xu, X. Chen, H. N. Kim and J. Yoon, *Chem. Soc. Rev*., 2010, **39**, 127.

3 C. Caltagirone and P.A. Gale, *Chem.Soc. Rev*., 2009, **38**, 520.

4 (a) H. G. Lee, J. H.Lee, S. P.Jang, I. H. Hwang, S.J. Kim, Y. Kim, C. Kim and R. G. Harriso, *Inorg. Chim. Acta.,* 2013, **394**, 542; (b) J. H. Kim, J. Y. Noh, I. H. Hwang, J. Kang, J. Kim and C. Kim,*Tetrahedron Lett,*. 2013, **54**, 2415; (c) J. Kang, H. K. Kang, H. Kim, J. Lee, E. J.Song, K.D. Jeong, C. Kim and J.Kim, *Supramol. Chem*., 2013, **25**, 65; (d) H.Y. Lin, P.Y. Cheng, C.F. Wan and A.T. Wu, *Analyst.,* 2012, **137**, 4415.

5 D.P. Perl and A.R. Brody, *Science.,* 1980, **208**, 297.

6 Z. Dai, N. Khosla and J.W. Canary, *Supramol. Chem,*. 2009, **21**, 296.

7 (a) B. Armstrong, C. Tremblay, D. Baris and G. Theriault, Am. J. Epidemiol., 1994, **139**, 250; (b) P.D. Darbre, *J. Inorg. Biochem*.2005, **99**, 1912.

8 C. Exley, L. Swarbrick, R.K. Gherardi and F.J. Authier, *Med. Hypothese.,* 2009, **72**, 135.

9 A.B.S. Poleo, *Environ. Pollut*., 1997, **96,** 129.

10 (a) E. Àlvarez, M. L. Fernández-Marcos, C. Monterroso and M. J. Fernández-Sanjurjo,. *Forest Ecol. Manage*., 2005, **211**, 227; (b) J. Barcelo, C. Poschenrieder, *Environ. Exp. Bot.* 2002, **48**, 75.

11 (a) N. E. W. Alstad, B. M. Kjelsberg, L. A. Vøllestad, E. Lydersen and A. B. S. Poléo, *Environ. Pollut*., 2005, **133**, 333; (b) E.Delhaize and P. R. Ryan, *Plant Physiol.,* 1995, **107**, 315; (c) J. Ren and H. Tian,. *Sensors*.,2007, **7**, 3166.

12 J. Barcelo and C. Poschenrieder, *Environ. Exp. Bot.,* 2002, **48**, 75. (b) B. Valeur and I. Leray, *Coord. Chem. Rev*., 2000, **205**, 3; (c) Z. Krejpcio and R. W. P. J. Wojciak, *Environ. Stud.,* 2002, **11**, 251.

13 (a) S. Guha, S.Lohar, A. Sahana, A. Banerjee, D. A. Safin, M. G. Babashkina, M. P. Mitoraj, M.l Bolte, Y. Garcia, S. K. Mukhopadhyay and D. Das, *Dalton Trans.,* 2013, **42**, 10198; (b) M. Mukherjee, S. Pal, S. Lohar, B. Sen, S. Sen, S. Banerjee, S. Banerjee and P. Chattopadhyay, *Analyst.,* 2014, **139**, 4828. (c) Z. Wang, M. A. Palacios and P. Anzenbacher, Jr. *Anal. Chem.,* 2008, **80**, 7451; (d) H. Shirase, Y. Mori, Y. Fukuda and M. Uchiyama, *Monatsh Chem*., 2009, **140**, 801.

14 (a) D. C Silcox and D. J. J. McCarty, *Clin. Invest*., 1973, **52**, 1863; (b) M. Ronaghi, S.Karamohamed, B.Pettersson, M. Uhlen and P. Nyren, *Anal. Biochem.,* 1996, **242**, 84; (c) S. K. Kim, D. H. Lee, J. N.Hong and J .Yoon, *Acc. Chem. Res.,* 2009, **42**, 23.

15 (a) C.P. Li, H. R. Ibrahim, Y.Sugimoto, , H. Hatta and T. J. Aoki, *Agric. Food. Chem.,* 2004, **52**, 5752; (b) P. K. Datta, A. C. Frazer, M. Sharratt and H. G. Sammons, *J. Sci. Food Agric*., 1962, **13**, 556.

16 (a) C .Beck, H. Morbach, M. Stenzel, H. Collmann, P.Schneider and H. J. Girschick, *Open Bone J*., 2009, **1**, 8; (b) M. Doherty, C. Becher, M.Regan and A.J. Ledingham, *J. Ann. Rheum. Dis.* 1996, **66**, 432; (c) A. E. Timms, Y.Zhang, R. G. Russell and M. A.Brown,*Rheumatology.,* 2002, **41**, 725.

17 (a) S. K. Kim, D. H. Lee, J. I. Hong and J.Yoon, *Acc. of Chem. Res.,* 2009, **42**, 23; (b) S. Anbu, S .Kamalraj, C. Jayabaskaran and P. S. Mukherjee, *Inorg. Chem.,* 2013, **52**, 8294; (c) T .Sakamoto, A .Ojida and I. Hamachi, *Chem. Commun,*. 2009, **141**, 141; (d) T. Cheng, T .Wang, W .Zhu, X .Chen, Y .Yang, Y .Xu and X. Qian, *Org. Lett,*. 2011, **13**, 3656.

18 (a) J. R . Lakowicz , Principle of fluorescence spectroscopy, 3rd ed. (b) A. P. de Silva, H. Q. N. Gunaratne, T. A .Gunnlaugsson, T. M. Huxley, C. P. McCoy, J. T.Rademacher and T. E. Rice and *Chem. Rev*., 1997, **97**, 1515; (c) B. Valeur, J. Bourson, J .Pouget and A. W.Czarnik,. Fluorescent Chemosensors for Ion and Molecule Recognition; ACS Symposium Series 538; American Chemical Society: Washington, DC, 1993.

19 (a) A. Sahana , A. Banerjee , S. Lohar, S. Das , I. Hauli , S. K. Mukhopadhyay, J. S.Matalobos and D. Das, *Inorganic Chimica Acta,* 2013, **398**, 64; (b) Y. Mia, Z. Caob, Y. Chena, S. Longb, Q. Xiea, D. Lianga,Z. Wenpinga and J. Xianga. *Sensors and Actuators B.*, 2014 , **192**, 164; (c) W.H.Dinga, D.Wanga, X.J. Zhenga, W.J. Dingb, J.Q. Zhengc,W.H. Mud, W. Caoa and L.P. Jin, *Sensors and Actuators B.*,2015, **209**,359.

20 A. K. Mahapatra, S. K. Manna, C. D. Mukhopadhyay and D. Manda, *Sensors and Actuators B.*, 2014*,* **200***,*123.

21 V. Kumar, A. Kumar, U. Diwan, Shweta, Ramesh, S.K. Srivastava and K.K. Upadhyay, *Sensors and Actuators B.,*2015, **207**, 650.

22 (a) S. Ameer-Beg, S. M. Ormson, R. G. Brown, P. Matousek, M. Towrie, E. T. J. Nibbering, P. Foggi and F. V. R. Neuwahl, *J. Phys. Chem. A.*, 2001, **105**, 3709; (b) A. Weller, Z. Elektrochem., 1956, **60**, 1144; (c) W. Chen, Y. Xing and Y. Pang, Org. Lett., 2011, **13**, 1362; (d) S. Lim, J. Seo and S. Y. Park, *J. Am. Chem. Soc*., 2006, **128**,14542.

23 (a) D. Maity and T. Govindaraju, *Eur. J. Inorg. Chem*., 2011, 5479. (b) J. Wu, W. Liu, X. Zhuang, F. Wang, P. Wang, S. Tao, X. Zhang, S. Wu and S. Lee, *Org. Lett*., 2007, **9**, 33; (c) Y. K. Jang, U. C. Nam, H. L. Kwon, I. H. Hwang and C. Kim, *Dyes Pigm*., 2013, **99**, 6.

24 (a) S. Sen, T. Mukherjee, B. Chattopadhyay, A. Moirangthem, A. Basu, J. Marek and P. Chattopadhyay, *Analyst*, 2012, **137**, 3975;(b) C. Chen, D. Liao, C. Wan and A. Wu, *Analyst*, 2013, **138**, 2527.

25 (a) M. Tarek, M. Zaki, L. F. M. Esmail, A. Y. El-Sayed and Z. Fresenius, Anal. Chem., 1988, 331, 607; (b) B. Bodenant, F. Fages and M. Delville, *J. Am. Chem. Soc*., 1998, **120**, 7511.

26 C. R. Lohani, J.M. Kim, S.Y. Chung, J. Yoon and K. H. Lee, *Analyst*, 2010, **135**, 2079.

27 M. Hosseini, M.R. Ganjali,M. Tavakoli, P. Norouzi , F.Faridbod, H. Goldooz and A. Badiei, *J Fluoresc.,* 2011, **21**,1509.

28 (a) A. D. Becke, J. Chem. Phys., 1993, 98, 5648; (b) C. Lee, W. Yang and R. G. Parr, Phys. Rev. B: Condens. Matter, 1988, 37, 785; (c) D. Andrae, U. Haeussermann, M. Dolg, H. Stoll and H. Preuss, Theor. Chim. Acta, 1990, 77, 123.

29 M. J. Frisch, G. W. Trucks, H. B. Schlegel, G. E. Scuseria, M. A. Robb, J. R. Cheeseman, G. Scalmani, V. Barone, B. Mennucci, G. A. Petersson, H. Nakatsuji, M. Caricato, X. Li, H. P. Hratchian, A. F. Izmaylov, J. Bloino, G. Zheng, J. L. Sonnenberg, M. Hada, M. Ehara, K. Toyota, R. Fukuda, J. Hasegawa, M. Ishida, T. Nakajima, Y. Honda, O. Kitao, H. Nakai, T. Vreven, J. A. Montgomery Jr., J. E. Peralta, F. Ogliaro, M. Bearpark, J. J. Heyd, E. Brothers, K. N. Kudin, V. N. Staroverov, T. Keith, R. Kobayashi, J. Normand, K. Raghavachari, A. Rendell, J. C. Burant, S. S. Iyengar, J. Tomasi, M. Cossi, N. Rega, J. M. Millam, M. Klene, J. E. Knox, J. B. Cross, V. Bakken, C. Adamo, J. Jaramillo, R. Gomperts, R. E. Stratmann, O. Yazyev, A. J. Austin, R. Cammi, C. Pomelli, J. W. Ochterski, R. L. Martin, K. Morokuma, V. G. Zakrzewski, G. A. Voth, P. Salvador, J. J. Dannenberg, S. Dapprich, A. D. Daniels, O. Farkas, J. B. Foresman, J. V. Ortiz, J. Cioslowski and D. J. Fox, Gaussian 09, Revision D.01, Gaussian, Inc., Wallingford CT, 2013.